Available online at www.sciencedirect.com
ScienceDirect
Applied Surface Science 254 (2008) 2629–2637
applied surface science
www.elsevier.com/locate/apsusc

Decomposition of thin titanium deuteride films; thermal desorption kinetics studies combined with microstructure analysis

Wojciech Lisowski [a,*], Enrico G. Keim [b,*], Zbigniew Kaszkur [a], Mark A. Smithers [b]

[a] *Institute of Physical Chemistry, Polish Academy of Sciences, Kasprzaka 44/52, PL-01-224 Warszawa, Poland*
[b] *MESA+ Research Institute, Central Materials Analysis Laboratory, University of Twente, P.O. Box 217, 7500 AE Enschede, The Netherlands*

Received 1 August 2007; received in revised form 30 September 2007; accepted 30 September 2007
Available online 5 October 2007

Abstract

The thermal evolution of deuterium from thin titanium films, prepared under UHV conditions and deuterated in situ at room temperature, has been studied by means of thermal desorption mass spectrometry (TDMS) and a combination of scanning electron microscopy (SEM), transmission electron microscopy (TEM) and X-ray diffraction (XRD). The observed Ti film thickness dependent morphology was found to play a crucial role in the titanium deuteride (TiD_y) film formation and its decomposition at elevated temperatures. TDMS heating induced decomposition of fine-grained thin Ti films, of 10–20 nm thickness, proceeds at low temperature (maximum peak temperature T_m about 500 K) and its kinetics is dominated by a low energy desorption (E_D = 0.61 eV) of deuterium from surface and subsurface areas of the Ti film. The origin of this process is discussed as an intermediate decomposition state towards recombinative desorption of molecular deuterium. The TiD_y bulk phase decomposition becomes dominant in the kinetics of deuterium evolution from thicker TiD_y films. The dominant TDMS peak at approx. T_m = 670 K, attributed to this process, is characterized by E_D = 1.49 eV.
© 2007 Elsevier B.V. All rights reserved.

PACS : 61.72.Dd; 68.37.Hk; 68.37.Lp; 68.43.Vx; 68.55.Jk; 82.30.Lp

Keywords: Titanium deuteride films; Thermal desorption; Microstructure; XPS

1. Introduction

Studies of titanium hydride (deuteride) decomposition are essential to improve the performance of Ti–H (Ti–D) compounds, well-known in the application of hydrogen storage media in catalytic and energetic reactions [1,2], or as material for the synthesis of fine-grained Ti-based alloys [3]. Amongst the various titanium hydride materials, for the applications interest, as powders [4–8], ingots [9], ribbons [10] and films [11–17], the films were found to be very useful material for fundamental studies of the Ti–H_2 interaction. The films can be investigated in situ just after their preparation under UHV conditions. Following this procedure the influence of oxygen contamination is minimized, which may otherwise affect both the formation of titanium hydride and its high-temperature decomposition. This may explain why the reported titanium hydride film properties were found to be different from the other hydride materials. TDMS measurements, applied very often to monitor thermal decomposition of the titanium hydride material [5,10,13,14,16], reveal that TiH_y films are completely decomposed at much lower temperatures than any other titanium hydride materials. Malinowski [12] investigated the thermal decomposition of titanium deuteride films, 230 nm thick, in UHV using Auger LVV and LMV peak shape analysis. The author found a complete titanium deuteride decomposition being realized significantly below 683 K, which is referred to in the Ti–H phase diagram [18] for this process. Ultra-thin (close to monolayer) Ti films evaporated on Ru(0 0 0 1) were found to be very active towards hydrogen forming TiH_3 species already at 140 K [19].

Thin titanium films are able to form the titanium hydrides of various stoichiometry, up to the limiting hydrogen–titanium ratio 2:1 in the dihydride system, due to hydrogen interaction at room temperature [11,13–15,17]. Similar ability to titanium hydride formation at room temperature was also reported for

* Corresponding authors. Tel.: +31 53 4895915.
E-mail addresses: wlis@ichf.edu.pl (W. Lisowski), e.g.keim@utwente.nl (E.G. Keim).

0169-4332/$ – see front matter © 2007 Elsevier B.V. All rights reserved.
doi:10.1016/j.apsusc.2007.09.095

titanium hydride powder but only after long time ball milling under a hydrogen atmosphere [4,6]. The hydride formed by the milling process was also found to be decomposed at a lower initial and final dehydrogenation temperature as compared to hydride powder prepared by traditional methods [4,6]. The origin of this experimental observation has been discussed in terms of a particle size effect on the hydrogenation–dehydrogenation process, and decomposition of such nanocrystalline titanium hydride powder was considered to occur in two-steps, as $TiH_2 \rightarrow TiH_x \rightarrow \alpha$-Ti, where $0.7 < x < 1.1$ [6]. Upon surveying the literature with regard to titanium hydride film formation and decomposition we found some experimental data suggesting a dual character of this process on thin films as well. A broad large TDMS peak of deuterium, being a superposition of at least two desorption states, has been observed by Nowicka et al. [13,14], but the nature of these TDMS states was not discussed in detail. On the other hand, Checchetto et al. [16] reported single-narrow-peak TDMS spectra of deuterium during thermal decomposition of titanium deuteride films of different thickness (75–300 nm). These films were however, deposited in deuterium atmosphere (8.5×10^{-2} Pa) on the Si(1 0 0) substrate maintained at temperatures in the range 423–723 K. These observations support the idea that the morphology of the Ti films can play a crucial role in the titanium hydride formation and its decomposition.

In this work, we present experimental data dealing with this idea. The results of our studies on the thermal decomposition of thin titanium deuteride films of various morphology, as reflected in different film thicknesses, are discussed. The kinetics of this process was monitored by means of TDMS measurements. From the TDMS data the energetic features of deuterium evolution from thin deuterated films can be determined. Moreover, both the temperature range in which total deuteride decomposition occurs, and the total amount of deuterium evolved due to this process can be estimated. The TDMS results are correlated with the surface and bulk film morphology, which was determined by a combination of SEM, TEM and XRD analyses, therefore allowing a meaningful discussion about the nature of the deuterium TDMS states appearing during thermal decomposition of titanium deuteride films.

2. Experimental

The TDMS experiments were performed in a glass UHV apparatus [20]. Titanium films of various thickness between 10 and 100 nm were deposited each time onto the clean glass wall of the spherical cell, which was kept constant at 273 K, by evaporation of a Ti wire (0.127 mm diameter, Johnson Mathey, grade I) wound around a tungsten heater (0.3 mm diameter). The pressure measured with an ionisation gauge during the Ti

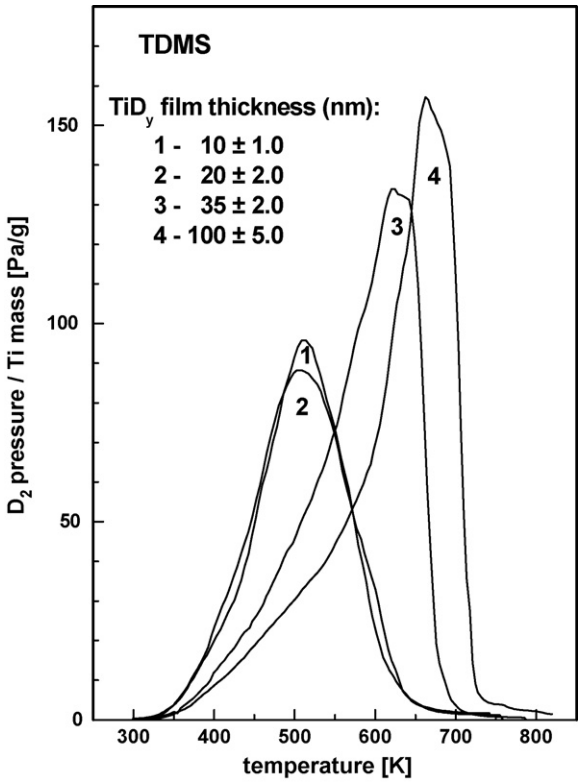

Fig. 1. Thermal desorption spectra of deuterium from titanium deuteride films of various thicknesses (for a description see legend). All films were prepared under the same experimental conditions, as the result of exposing Ti films at room temperature to the final deuterium equilibrium pressure of 1 Pa.

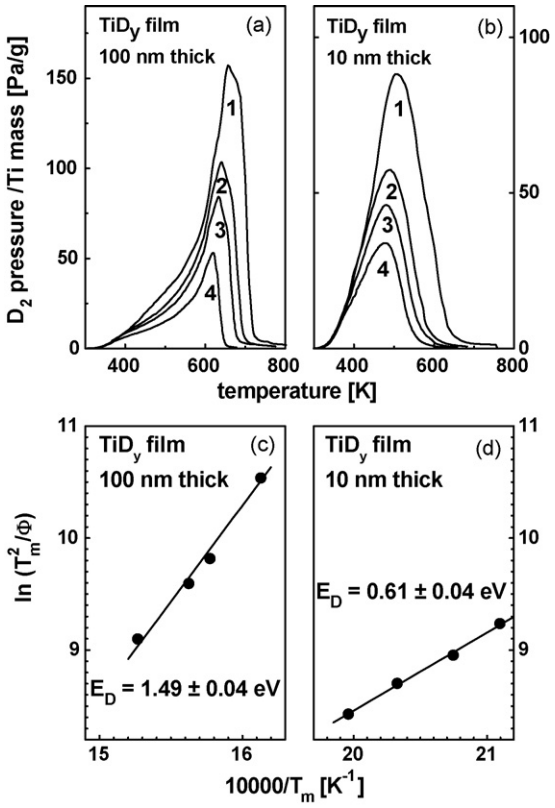

Fig. 2. Evaluation of the activation energy of deuterium evolution from titanium deuteride films of 100 and 10 nm thickness using the Kissinger method [24]. (a) TDMS spectra from the 100 thick TiD_y film, recorded at a heating rate of 48, 28, 22 and 11 K/min for spectra 1, 2, 3 and 4, respectively. (b) TDMS spectra from the 10 thick TiD_y film, recorded at a heating rate of 54, 40, 30 and 22 K/min for spectra 1, 2, 3 and 4, respectively. (c) and (d) Examination of the Kissinger Eq. (1) for the TDMS spectra in (a) and (b), respectively.

film deposition was lower than 1×10^{-7} Pa. After evaporation the films were annealed at 650 K for 60 min.

The titanium deuteride (TiD_y) films were obtained in situ due to interaction of thin Ti films with spectroscopically pure deuterium additionally purified by diffusion through a palladium thimble. Deuterium was introduced in successive, calibrated doses at 298 K until an equilibrium pressure of approximately 1 Pa was reached. The deuterium pressure was measured during adsorption by means of a MacLeod manometer to avoid atomisation of deuterium on the hot filament of the ionisation gauge. The amount of sorbed deuterium was determined in this work by means of the volumetric method and compared with the TDMS calculations [21]. The agreement was within ±5%. Upon knowing the mass of the Ti film and the deuterium uptake we could estimate an average atomic ratio D/Ti for all investigated TiD_y films. The atomic composition of the titanium hydride formed in thick (150–200 nm) Ti films exposed to hydrogen in the same experimental way was confirmed previously using SIMS analysis [17].

Morphological and structural examination of the Ti and TiD_y films was performed ''ex situ'' in separate analytical systems. Preparation of all films was however, performed in a glass UHV apparatus at the same conditions as in the TDMS experiment. Each time thin Ti films were deposited onto a clean, quartz substrate plate (5 mm × 8 mm in size and 1 mm thick), placed within the glass TDMS cell. The preparation procedure preceding TDMS was subsequently repeated ''in situ'' each time for a new sample. In this way we were able to prepare specimens representative of the Ti films used in the TDMS measurements after annealing at 650 K and after deuterium sorption at 298 K, respectively.

SEM (LEO Gemini 1550 FEG SEM) was carried out to study the surface morphology of the films. Cross-sectional TEM (XTEM) analysis (Philips CM300ST-FEG (S)TEM), on the other hand, was performed to obtain information regarding the bulk structure of corresponding films as well as to reveal the nanostructures formed in the surface region and the (Ti)TiD_y/quartz substrate interface. Small-spot micro diffraction analysis allowed the crystal phases in the bulk of the Ti and TiD_y films to be identified. The TEM specimens of both types of films were prepared in cross-section according to the recipe described previously [22].

XRD analyses provided useful information with regard to the titanium deuterated film composition and crystallite sizes of both the Ti and TiD_y phases. The XRD diffraction data were collected using the standard Siemens D 5000 diffractometer.

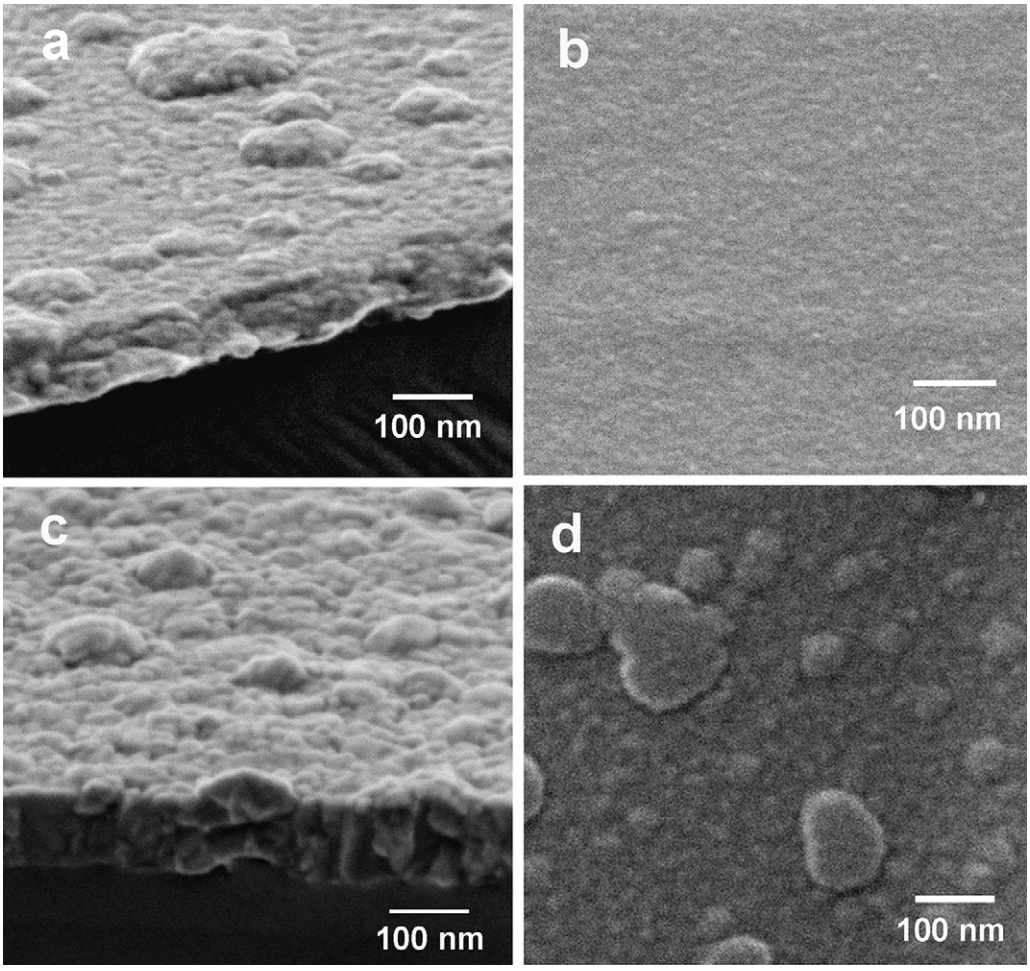

Fig. 3. SEM images of a (a) 100 nm thick Ti film surface (cross-section view), (b) 20 nm thick Ti film surface (surface view), (c) 100 nm thick TiD_y film surface (cross-section view), (d) 20 nm thick TiD_y film surface (surface view).

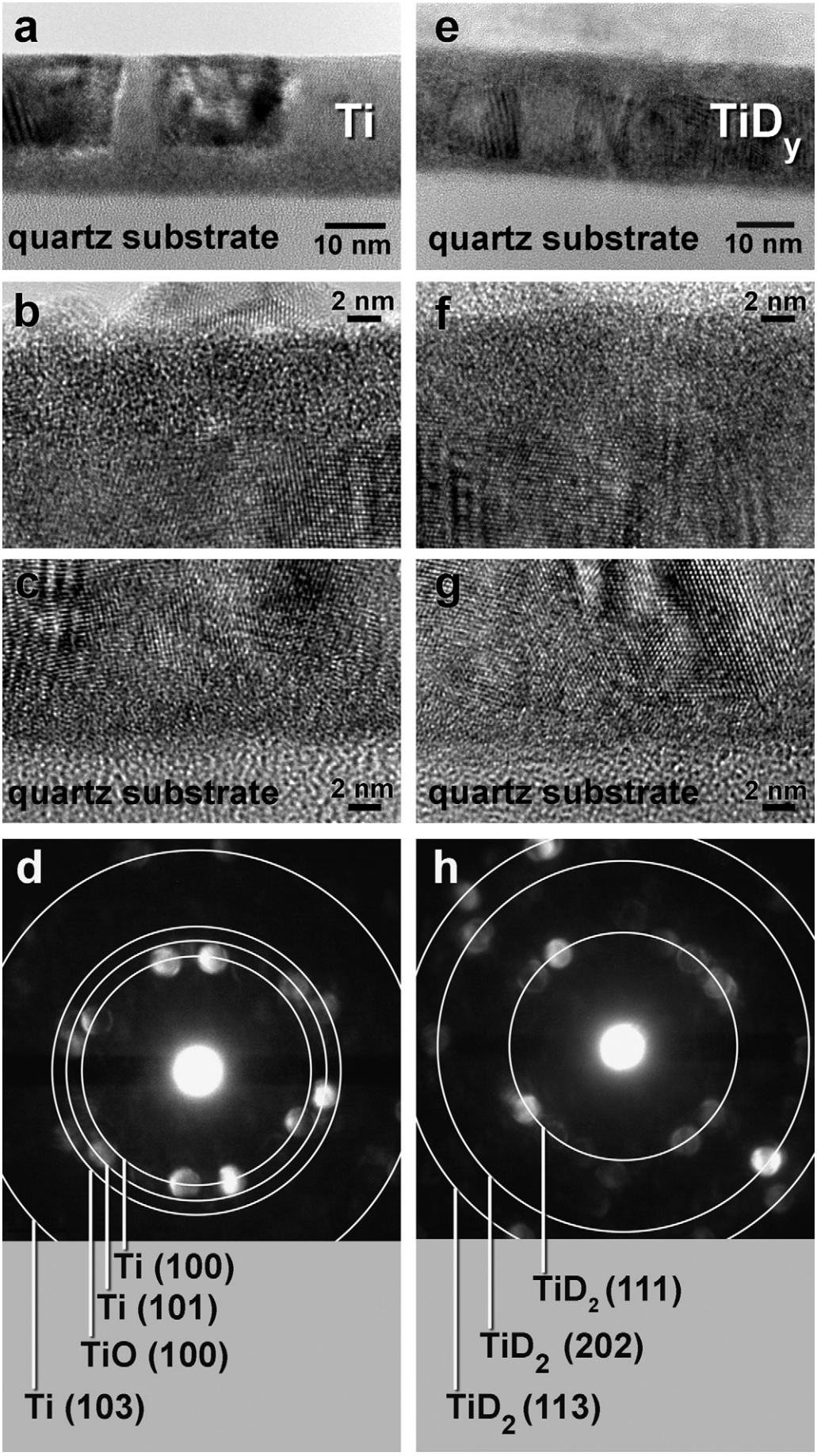
a
Ti
quartz substrate
10 nm
e
TiD$_y$
quartz substrate
10 nm
b
2 nm
f
2 nm
c
quartz substrate
2 nm
g
quartz substrate
2 nm
d
Ti (100)
Ti (101)
TiO (100)
Ti (103)
h
TiD$_2$ (111)
TiD$_2$ (202)
TiD$_2$ (113)

The average size of metal crystallites was determined from the Scherrer's equation [23] using the integral width of selected XRD reflections fitted to the analytical Pearson VII functions.

3. Results

3.1. Thermal desorption studies

Fig. 1 shows the TDMS spectra for deuterium from thin titanium films of various thicknesses being exposed to deuterium at the same experimental conditions. On all films maintained at 298 K, deuterium was introduced in successive calibrated doses until the same final D_2 pressure of 1.0 Pa was reached. After adsorption deuterium was evacuated from the gas phase to the final pressure approaching 10^{-4} Pa, which was the starting point of each TDMS experiment.

TDMS spectra reveal that the kinetics of deuterium evolution from thin TiD_y films is different from that, observed on titanium deuteride films thicker than 30 nm. The broad spectrum with a maximum peak temperature T_m of about 500 K and only a trace overlapped peak at about 550–600 K appear for deuterium evolution from the TiD_y films with a thickness below 20 nm (spectra 1 and 2 in Fig. 1). The thermal desorption spectra recorded from thicker TiD_y films (spectra 3 and 4 in Fig. 1) exhibit a complex character with T_m shifted from 630 to 670 K as the film thickness increases from 35 to 100 nm. The broad asymmetric spectra disclose evolution of deuterium in various overlapping TDMS states.

From an analysis of the TDMS spectra both the amount of desorbed deuterium and the energy necessary for activation of deuterium desorption can be estimated. The average atomic ratio D/Ti for TiD_y films with a thickness of 100, 35, 20, and 10 nm, is 1.99, 1.78, 1.13, and 1.15, respectively.

In order to estimate an activation energy for deuterium evolution from thick and thin titanium deuteride films we analysed in separate experiments the thermal decomposition of two TiD_y films, 100 nm and 10 nm thick (see spectra in Fig. 2a and b, respectively), using the Kissinger method [24]. Following this method the TDMS spectra were recorded at various heating rates. The observed shift of peak temperatures with heating rate has been used to determine the activation energy for deuterium evolution from both types of films according to the Kissinger relation [24]:

$$\ln\left(\frac{T_m^2}{\Phi}\right) = \frac{E_D}{RT_m} + A \quad (1)$$

where T_m denotes the maximum temperature, E_D is the activation energy of deuterium evolution, Φ is the heating rate, R is a gas constant and A is a constant.

The activation energies have been estimated from the plots of $\ln(T_m^2/\Phi)$ against $1/T_m$, which are presented in Fig. 2c and d for thick and thin TiD_y films, respectively. The E_D values derived from this plot for 100 nm thick and 10 nm thick TiD_y films are 1.49 ± 0.04 eV and 0.61 ± 0.04 eV, respectively. These values indicate a different nature of the deuterium evolution process in thin and relatively thick TiD_y films.

3.2. SEM analysis of Ti and TiD_y film surface morphology

Fig. 3 shows the SEM images of the Ti and TiD_y film surfaces. The surface morphology of both films, about 20 nm and 100 nm thick, are compared. The 100 nm thick Ti film (Fig. 3a) is characterized by a fine-grained (25–40 nm) surface morphology. Small grains are well separated but also aggregate into larger clusters (80–300 nm). Smooth and super fine-grained (10 ± 2 nm) surface morphology is attributed to the 10–20 nm thick Ti film (Fig. 3b). A distinct change in the Ti film surface morphology has been observed after deuterium treatment leading to TiD_y formation (Fig. 3c and d for the thick and thin film, respectively). Both thick and thin Ti films become more rough. The thin TiD_y film surface (Fig. 3d) reveals also clusters (25–100 nm) as a result of aggregation of very fine TiD_y grains.

3.3. Cross-sectional TEM analysis of thin Ti and TiD_y films

The results of TEM analysis of the bulk structure of thick Ti and TiD_y films (thicker than 100 nm) were reported previously [25]. The cross-section TEM images revealed a polycrystalline structure in both films with polygonal and columnar grains as well as distinct coarsening of the surface and subsurface region of the TiD_y film. In the present paper, we use the combination of XTEM and small-spot micro diffraction analysis to obtain information regarding the bulk structure of the 20 nm thick Ti and TiD_y films. The results are shown in Fig. 4. In the left column a set of low- and high-magnification cross-section TEM images of the Ti film is shown together with the micro diffraction pattern recorded on this area (diameter analysed area approximately 2 nm). In the right column the corresponding images for the TiD_y film are compared. Low-magnification TEM cross-sectional images of Ti (a) and TiD_y (e) films reveal a heterogeneous structure in both films including amorphous areas and polycrystalline grains (8–12 nm). The amorphous character of both thin films is very distinct at the top and bottom of cross-section areas of Ti (b and c) and TiD_y (f and g) films.

Fig. 4d and h show typical micro diffraction patterns from polycrystalline grains in the Ti and TiD_y films, respectively. From a direct measurement of the radius between the central spot and the diffraction spots lying on artificial concentric

Fig. 4. TEM data for 20 nm thick titanium (left column) and titanium deuteride (right column) films. Low-magnification TEM cross-sectional bright-field images of both films are presented for Ti (a) and TiD_y (e). High-magnification TEM cross-sectional lattice images illustrating the surface region of both films are shown in (b) for Ti and in (f) for TiD_y; corresponding lattice images focusing on the interface between the quartz substrate and film are presented in (c) for Ti and (g) for TiD_y. The micro diffraction patterns recorded on the Ti and TiD_y areas (beam diameter approximately 2 nm) are shown in images (d) and (h), respectively, together with the assignment of the most relevant low-index Miller planes of the diffraction spots.

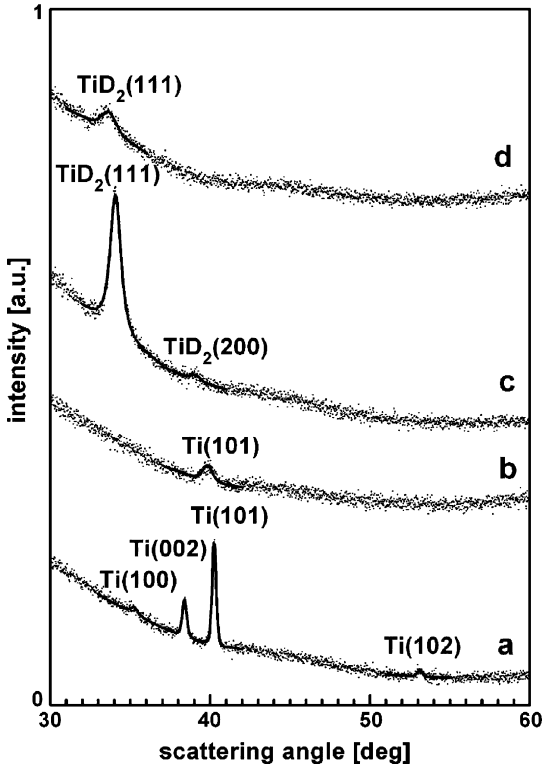

Fig. 5. XRD diffractograms of a 100 nm thick Ti film (pattern (a)), 20 nm thick Ti film (pattern (b)), 100 nm thick TiD_y film (pattern (c)), 20 nm thick TiD_y film (pattern (d)).

circles (in Fig. 4d and h shown as semitransparent grey circle sections drawn through the relevant diffraction spots), the Miller index planes could be determined. From the micro diffraction patterns the most relevant crystallographic planes belonging to the Ti hcp and TiD_2 fcc structure could be identified [26]. In Ti (Fig. 4d) we were also able to detect a weak diffraction spot associated with titanium oxide [26].

3.4. XRD analysis

XRD analysis of 20 nm and 100 nm thick titanium films, after exposure to deuterium at room temperature, has been performed in order to characterize the crystalline phases of both deuterated films. In Fig. 5 XRD diffractograms are presented taken from these films, which are compared to XRD diffractograms of corresponding Ti films. A set of distinct peaks, characteristic for Ti hcp [26], was observed for the 100 nm thick Ti film (Fig. 3a) and only one small peak, referred to as Ti(1 0 1), was detected for the 20 nm thick Ti film (Fig. 3b). The corresponding XRD patterns for titanium films deuterated under UHV conditions (c and d, respectively) exhibit the fcc CaF_2-like structure of the titanium deuteride (δ-phase TiD_2) [26] with a dominant (1 1 1) orientation. No titanium oxide phase was observed. A rough estimation of the grain size has been performed from the full width at half maximum of the XRD peaks using the Scherrer formula [23], and results are presented in Table 1. Small grain sizes of similar magnitude were observed in both Ti and TiD_y thin films, and in the thick TiD_y film.

Table 1
Mean crystallite size evaluated from XRD diffraction peaks of the Ti and TiD_y films (Fig. 5) using Scherrer formula [23]

Material	Film thickness (nm)	Crystallite size (nm)
Ti film	100 ± 5	29.8
Ti film	10 ± 1	9.7
TiD_y film	100 ± 5	10.3
TiD_y film	10 ± 1	7.3

4. Discussion

4.1. Deuterium desorption from thin TiD_y films

The low E_D value, attributed to deuterium desorption from thin TiD_y films is close to the activation energy for hydrogen desorption from δ-TiH_2 powder (0.65 eV), found recently by Sandim et al. [8]. On the other hand, this value is similar to the heat of hydrogen solution in Ti (0.57 eV) [27] and also to the activation energy of deuterium diffusion E_{diff} in titanium deuteride (0.6–0.67 eV) [28,29]. The diffusion mechanism of deuterium migration within Ti and titanium hydride materials has been investigated by several authors [28–31]. In Table 2 we present some selected data related to the deuterium diffusion in Ti and TiD_y materials. Analysing this data allows us to determine if diffusion can be a rate-limiting process of the TiD_y film decomposition.

Assuming the diffusion concept, one can roughly estimate a diffusion length L_{diff} of deuterium atoms desorbing within one TDMS peak using the relation [32]:

$$L_{diff} \approx \left(\frac{D_{diff} \Delta T}{\Phi} \right)^{1/2} \quad (2)$$

where D_{Diff} is the diffusion coefficient of deuterium atoms for a temperature at the TDMS peak maximum (T_m), ΔT is the full width at half maximum (FWHM) of the TDMS peak and Φ is the heating rate. For calculations we took the D_{Diff} data reported for the TiH_y powder (Table 2), which particle size was found [4,6] to be close to the mean crystallite size of our thin TiD_y film (Table 1). Taking a value of $D_{Diff} = 7.7 \times 10^{-14}$ m^2/s, $\Delta T = 150$ K as measured at $T_m = 500$ K of the TDMS peak 1 (Fig. 1), and $\Phi = 0.8$ K/s, one can estimate L_{diff}, using Eq. (2), to be ≈3800 nm. This value is almost 400 times larger than the actual thickness of the TiD_y film. From the consideration mentioned above it is safe to conclude that diffusion as the rate-limiting process in the TDMS kinetics can be excluded.

We support the idea that the fast diffusion transport of deuterium atoms through the bulk of the TiD_y film is moderated at the surface, leading to a relative increase of atomic deuterium concentration at the surface and subsurface region of the Ti film. This assumption agrees with a surface energy model for the Ti–H_2 system proposed by Brown and Buxbaum [33], in which a surface energy barrier limits the migration of deuterium atoms within a surface-bulk interface region. That can result in a temporary accumulation of deuterium atoms within the surface-subsurface area. Such a state of deuterium

Table 2
Diffusion parameters of deuterium in Ti and TiD_y systems

Diffusion system	D_0 ($m^2\ s^{-1}$)	E_{diff} (eV)	T (K)	References
D in β-Ti	2.63×10^{-7}	0.28	1173–1473	[29]
D in α-Ti	2.75×10^{-7}	0.43	873–1298	[29,30]
D in $TiH_{1.98}$ powder	9.4×10^{-8}	0.67	690–820	[27]
D in $TiH_{1.74}$ powder	1.08×10^{-7}	0.60	620–800	[27]
D in $TiH_{1.5}$ foil	–	0.60	240–340	[28]

species can be considered as the intermediate state, which reconstructs as a result of recombinative interaction of deuterium surface adatoms and desorption into the gas phase.

In order to analyze the intermediate character of this state we used the intermediate kinetic model for desorption derived by King [34]. The model assumes that desorption, being a reversal process to adsorption, must be involved in a transfer through the intermediate state to the gas phase. In this model, by analogy with Kisliuk's precursor state model for adsorption kinetics [35], only a fraction F of the molecules transferred from the chemisorption state to the intermediate state is scattered into the gas phase and hence desorbed. Thus the rate of desorption of this state can be expressed as [34]:

$$-\frac{dC_D}{dt} = -F\nu C_D \exp\left(-\frac{E_d}{RT}\right) \quad (3)$$

where C_D is a relative concentration of deuterium in the intermediate state. $C_D = 1$ for a total amount of deuterium desorbed within a low-temperature TDMS peak.

The term F was derived as total probabilities of desorption of the intermediate state and can be written as [34,36]:

$$F = f_d + f_m\left[1 - \frac{s_0}{\alpha}\left(1 + K\frac{C_D}{1 - C_D}\right)^{-1}\right] \quad (4)$$

where f_d is the probability of scattering into the gas phase, f_m is the probability of hopping to a neighbouring site, s_0 is the sticking probability at zero coverage, α is the condensation coefficient and K is a parameter independent of C_D, showing the relation between the probability of adsorption, migration and desorption of the intermediate state [34].

From an analysis of the experimentally determined course of dC_D/dt as a function of T (Fig. 6a) using Eq. (3) one can calculate the $F\nu$ values as a function of C_D. In our calculations we use $E_D = 0.61$ eV, estimated from an analysis based on the Kissinger relation (Eq. (1), and Fig. 2(b and c)). The data points $F\nu = f(C_D)$ experimentally determined (see the marked points in Fig. 6b) were compared to various $F(C_D)\nu$ spectra computed from Eq. (4) with various K parameter values and using reasonable values for the precursor state parameters [34,37]. As a result the $F\nu = f(\theta_A)$ spectrum computed for $K = 0.02$ and $\nu = 2.5 \times 10^7$, $f_d = 10^{-2}$, $f_m = 1$, and $s_0/\alpha = 1$, was found to be the best fit of the experimental data points (see the continuous curve in Fig. 6b). All specified terms are assumed to be independent of temperature over the range where desorption occurs. Such low values of the K parameter indicate that the term F strongly depends on the deuterium concentration and that the influence of the intermediate state on desorption kinetics is highly probable.

4.2. Thick TiD_y film decomposition

Two different stages for deuterium evolution can be distinguished in the TDMS spectrum as a result of thermal decomposition of TiD_y films, thicker than 30 nm (Fig. 1). The low-temperature part of the spectrum, which originates from the desorption process of the thinnest films (<20 nm), is followed by a dominant peak at about 650 K. This peak can be assigned to the decomposition of the TiD_2 phase. Supporting evidence is given by both the measured activation energy for desorption E_D (1.49 eV) and the TDMS peak temperature. The E_D value agrees favourably with data reported in literature for

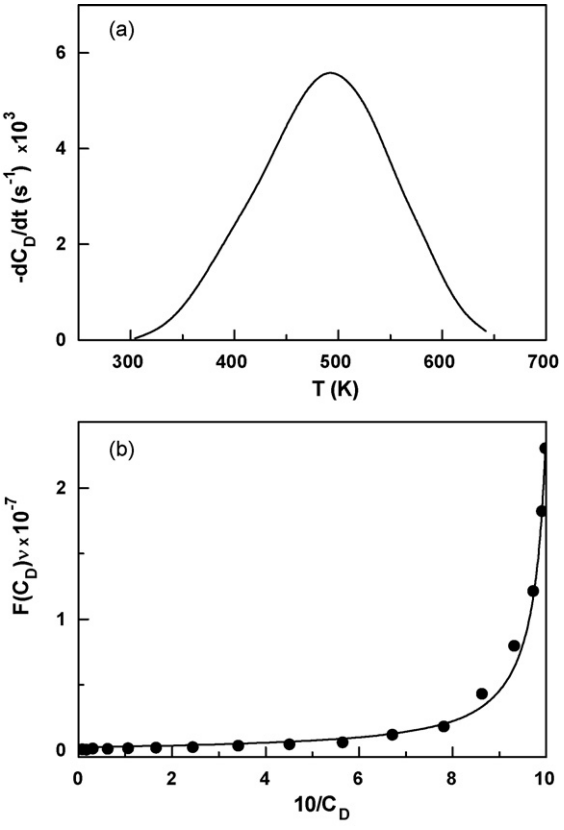

Fig. 6. (a) Experimental course of $-dC_D/dt = f(T)$. (b) Examination of the $F\nu = f(C_D)$ dependence. The points represent the $F\nu$ term values calculated from (a) using Eq. (3). The lines represent the computed course of $F\nu = f(C_D)$ using Eq. (4) and $K = 0.02$, $\nu = 2.5 \times 10^7\ s^{-1}$, $f_d = 10^{-2}$, $f_m = 1$, $s_0/\alpha = 1$.

deuterium desorption from titanium films deuterated at high-temperature (1.53–1.63 eV) [16] and for decomposition of TiH_2 powder (1.37 eV) [6].

The dominant TDMS peak is observed within a temperature range close to 573 K reported for the eutectoid phase transformation $(\alpha + \delta) \leftrightarrow \beta$ in the Ti–H_2 system [18]. If we assume that this temperature is also specific for the TiD_2 phase decomposition in our films, we can estimate a relative contribution of this process to the total TDMS heating induced deuterium evolution from thin and thick TiD_y films. For this purpose we compared the deuterium contents remaining in the TiD_y films at 573 K during TDMS heating; the results are presented in Fig. 7. It can be seen that a relative atomic concentration of deuterium atoms at this temperature (see dashed line in Fig. 7) in the 100 nm thick TiD_y film exceeds 60% whereas in 10–20 nm thick films this value is lower than 12%. It is important to note that in spite of the relatively low concentration of deuterium in thin TiD_y films, XRD and XTEM diffraction provide evidence of a crystalline TiD_2 phase in these films (see Fig. 4h and Fig. 5d). Therefore, the atomic ratio parameter D/Ti, evaluated from volumetric and TDMS data is not suitable for specific TiD_y phase identification. However, taking into account a high content of deuterium in the thick TiD_y film at 573 K, a relatively high contribution of the TiD_2 phase in the bulk structure of thick TiD_y films at this stage of the thermal desorption process is expected.

A two-step decomposition process of the titanium hydride phase was considered also by other authors. Takasaki et al. [9] estimate the activation energy of δ-hydride phase dissociation and hydrogen evolution from electrochemically charged Ti to be about 1.1 eV and 0.51 eV, respectively. Bhosle et al. [6] considered the decomposition of TiH_2 powder as a two-step process. In this model dehydrogenation of TiH_2 occurs through the metastable TiH_y (for $y = 0.7$–1.1) phase formation ($E_D = 1.37$ eV), which is then transformed into α-Ti ($E_D = 0.77$ eV). Both evaluated E_D values, attributed to these processes agree favourably with our TDMS data.

4.3. Correlation of TDMS spectra with titanium deuteride film morphology

Taking into account the experimental data presented above we can formulate some observations correlating the morphology of the titanium deuteride films with the TDMS data: (i) TDMS spectra reveal relatively low deuterium concentrations in (10–20) nm thick TiD_y films as compared to the thicker films, (ii) SEM/TEM images and XRD measurements show comparable small grain size morphology in all TiD_y films, on average a small grain size in thin Ti films and larger grain sizes in thicker films (Table 1), (iii) large grain size Ti films are more active towards deuterium at room temperature forming TiD_y films with high deuterium content (y value close to 2), (iv) thin Ti films, containing very fine grains (about 10 nm), transform into titanium deuteride films with lower deuterium concentrations (y value 1.0–1.2) but decomposition of such TiD_y films occur at much lower temperature than decomposition of corresponding thick films.

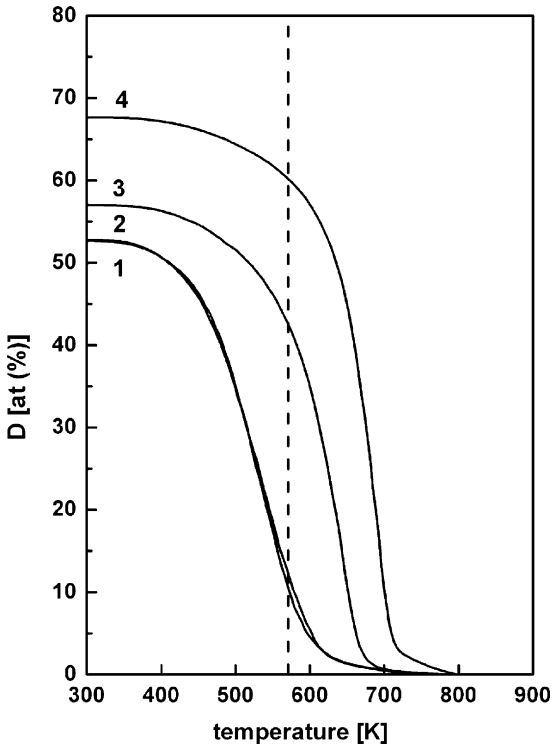

Fig. 7. Atomic concentration of deuterium atoms in the titanium deuteride films with thickness 10, 20, 35 and 100 nm (see lines 1, 2, 3, and 4, respectively) as a function of the TDMS heating temperature. The dashed line shows the atomic concentration of deuterium at 573 K (see text for details).

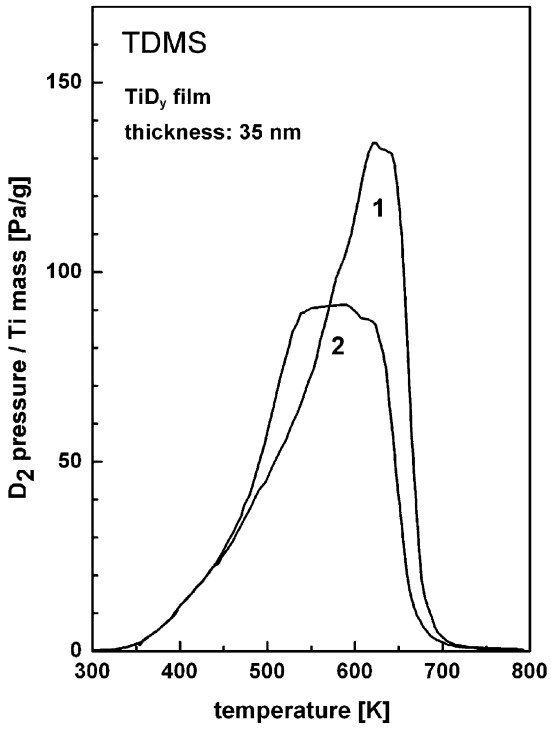

Fig. 8. TDMS spectra of deuterium from a 35 nm thick titanium deuteride film illustrating the influence of the deuteride–dedeuteride process recycling. Spectrum (1) was taken after a single process of RT Ti exposure to deuterium. Spectrum (2) was recorded on the same film after three successive cycles of titanium deuteride formation and decomposition.

The last mentioned phenomenon, related to thin Ti–TiD_y film transformation, is similar to that observed during the TiH_2 powder formation by ball milling at room temperature and its high-temperature dehydrogenation [4,6]. Extended time ball milling of TiH_2 powder was found to reduce the powder particle size (to 8 nm), to decrease the hydrogen content (y value 0.7–1.1) and shift the transformation peak to lower temperatures [6].

Reduction of the Ti grain size can also be realized by the hydride–dehydride process leading to applications in the synthesis of fine-grained Ti-based alloys [3]. We applied this phenomenon to show how the change in grain size film morphology affects features in the TDMS spectra of deuterium as a result of the TiD_y film decomposition. For this purpose the process of titanium deuteride formation at room temperature followed by its thermal decomposition was repeated three times using the same, 35 nm thick, Ti film. The TDMS spectra recorded after the first and the third deuteride–dedeuteride process are shown in Fig. 8 (spectra (1) and (2), respectively). One can see significant broadening of the TDMS spectrum (2) and a shift to lower temperatures. Deuterium contents decrease by approximately 13%. It appears that recycling the deuteride–dedeuteride process, involving a reduction in the grain size of the Ti film, activates the low-temperature processes of the TDMS controlled titanium deuteride film decomposition.

5. Conclusions

Titanium deuteride films of various thicknesses can be easily formed in UHV conditions at room temperature. Deuterium contents of these films have been found to be closely related to the morphology of the Ti film, being different for various film thicknesses. The average grain size for Ti films, 10 nm and 100 nm thick, was evaluated from XRD and TEM/SEM data, and found to be about 10 and 30 nm, respectively. Following the same deuterium treatment procedure, fine-grained thin Ti films, 10–20 nm thick, were found to form a titanium deuteride (TiD_y) phase showing a lower deuterium content than in thicker films.

Decomposition of the TiD_y films has been investigated using the thermal desorption method. The TDMS spectra of deuterium disclose a complex character of the kinetics of thermally induced deuterium evolution from thin TiD_y films of various thicknesses. Deuterium evolution from TiD_y films, thinner that 30 nm, proceeds at low temperature and is dominated by a process, which is activated with low energy ($E_D = 0.61$ eV). The origin of this process is discussed as an intermediate state of deuterium decomposition from surface and subsurface areas of the Ti film towards molecular desorption of deuterium. Decomposition of thicker TiD_y films is additionally complicated by bulk phase decomposition becoming dominant at temperatures in excess of 550 K. The dominant TDMS peak at $T_m \approx 670$ K, attributed to this process, is characterized by $E_D = 1.49$ eV.

References

[1] D.G. Westlake, C.B. Satterthwaite, J.H. Weaver, Phys. Today 31 (1978) 32.
[2] Y. Hirooka, J. Vac. Sci. Technol. A 2 (1984) 16.
[3] K.I. Moon, K.S. Lee, J. Alloys Compd. 264 (1998) 258.
[4] H. Zhang, E.H. Kisi, J. Phys. Condens. Matter. 9 (1997) L185.
[5] F. von Zeppelin, M. Hirscher, H. Stanzick, J. Banhart, J. Comp. Sci. Technol. 63 (2003) 2293.
[6] V. Bhosle, E.G. Baburaj, M. Miranova, K. Salama, Mater. Eng. A 356 (2003) 190.
[7] V. Bhosle, E.G. Baburaj, M. Miranova, K. Salama, Metall. Mater. Trans. 34A (2003) 2793.
[8] H.R.Z. Sandim, B.V. Morante, P.A. Suzuki, Mater. Res. 8 (2005) 293.
[9] A. Takasaki, Y. Furuya, K. Ojima, Y. Taneda, J. Alloys Compd. 224 (1995) 269.
[10] J.A. Schwarz, R.S. Polizzotti, J.J. Burton, Surf. Sci. 67 (1977) 10.
[11] G. Wedler, H. Strothenk, Z. Phys. Chem. Neue Folge 48 (1966) 86.
[12] M.E. Malinowski, J. Vac. Sci. Technol. 16 (1979) 962.
[13] E. Nowicka, Z. Wolfram, W. Lisowski, R. Duś, Appl. Surf. Sci. 93 (1996) 53.
[14] E. Nowicka, R. Duś, Langmuir 12 (1996) 1520.
[15] W. Lisowski, A.H.J. van den Berg, M. Smithers, Surf. Interface Anal. 26 (1998) 213.
[16] R. Checchetto, L.M. Gratton, A. Miotello, A. Tomasi, P. Scardi, Phys. Rev. B 58 (1998) 4130.
[17] W. Lisowski, A.H.J. van den Berg, D. Leonard, H. Mathieu, J. Surf. Interface Anal. 29 (2000) 292.
[18] J.L. Murray, in: T.B. Massalski (Ed.), Binary Alloy Phase Diagrams, American Society of Metals, Metals Park, Ohio, 1986, p. 1878.
[19] J.P.S. Badayal, A.J. Gellman, R.M. Lambert, J. Catal. 111 (1988) 383.
[20] W. Lisowski, Vacuum 54 (1999) 13.
[21] W. Lisowski, E.G. Keim, M.A. Smithers, J. Vac. Sci. Tech. A 21 (2003) 545.
[22] W. Lisowski, E.G. Keim, M. Smithers, Appl. Surf. Sci. 189 (2002) 148.
[23] A.L. Patterson, Phys. Rev. 56 (1939) 978.
[24] H.E. Kissinger, Anal. Chem. 29 (1957) 1702.
[25] W. Lisowski, E.G. Keim, A.H.J. van den Berg, M.A. Smithers, Anal. Bioanal. Chem. 385 (2006) 700.
[26] Powder Diffraction File, Joint Committee on Powder Diffraction Standards, ICDD, 1999, Ti: card 44-1294, $TiH_{1.971}$: card 07-0370, $TiH_{0.71}$: card 40-0980, TiO: card 85-2084.
[27] R.C. Brouwer, R. Griessen, Phys. Rev. B 40 (1989) 1481.
[28] U. Kaess, G. Majer, M. Stoll, D.T. Peterson, R.G. Barnes, J. Alloys Compd. 259 (1997) 74.
[29] H. Wipf, B. Kappesser, R. Werner, J. Alloys Compd. 310 (2000) 190.
[30] S. Naito, M. Yamamoto, M. Doi, M. Kimura, J. Electrochem. Soc. 145 (1998) 2471.
[31] S. Naito, M. Yamamoto, T. Miyoshi, M. Mabuchi, M. Doi, M. Kimura, J. Chem. Soc. Faraday Trans. 92 (1996) 3407.
[32] Y.S. Nechaev, O.K. Alexeeva, Int. J. Hydrogen Energy 28 (2003) 1433.
[33] C.C. Brown, R.E. Buxbaum, Metall. Trans. A 19 (1988) 1425.
[34] D.A. King, Surf. Sci. 64 (1977) 43.
[35] P.J. Kisliuk, J. Phys. Chem. Solids 3 (1957) 95;
P.J. Kisliuk, J. Phys. Chem. Solids 5 (1958) 78.
[36] D.A. King, in: R. Vanselow (Ed.), Chemistry and Physics of Solid Surfaces, vol. 2, CRC Press, Boca Raton, 1976, p. 87.
[37] C.O. Steinbrüchel, Surf. Sci. 51 (1975) 539.